BIOCHEMICAL PHARMACOLOGY 75 (2008) 1198–1208

available at www.sciencedirect.com

ScienceDirect

journal homepage: www.elsevier.com/locate/biochempharm

Binding thermodynamic characterization of human $P2X_1$ and $P2X_3$ purinergic receptors

Katia Varani [a], *Annmarie Surprenant* [b], *Fabrizio Vincenzi* [a], *Alice Tosi* [a], *Stefania Gessi* [a], *Stefania Merighi* [a], *Pier Andrea Borea* [a,*]

[a] *Department of Clinical and Experimental Medicine, Pharmacology Unit, University of Ferrara, via Fossato di Mortara 17–19, 44100 Ferrara, Italy*

[b] *Faculty of Life Science, University of Manchester, Manchester M13 9PT, United Kingdom*

ARTICLE INFO

Article history:
Received 4 September 2007
Accepted 31 October 2007

Keywords:
$P2X_1$ and $P2X_3$ purinergic receptors
HEK 293 cells
[^{3}H]αβmeATP binding
Binding thermodynamics
Enthalpy–entropy compensation
Agonist–antagonist discrimination

ABSTRACT

The present study was designed to perform binding and thermodynamic characterization of human $P2X_1$ and $P2X_3$ purinergic receptors expressed in HEK 293 cells. The thermodynamic parameters ΔG°, ΔH° and ΔS° (standard free energy, enthalpy and entropy) of the binding equilibrium of well-known purinergic agonists and antagonists at $P2X_1$ and $P2X_3$ receptors were determined. Saturation binding experiments, performed in the temperature range 4–30 °C by using the high affinity purinergic agonist [^{3}H]αβmeATP, revealed a single class of binding sites with an affinity value in the nanomolar range in both cell lines examined. The affinity changed with the temperature whereas receptor density was essentially independent of it. van't Hoff plots of the purinergic receptors were linear in the range 4–30 °C for agonists and antagonists. The thermodynamic parameters of the $P2X_1$ or $P2X_3$ purinergic receptors were in the ranges $-31\ \text{kJ mol}^{-1} \leq \Delta H^\circ \leq -19\ \text{kJ mol}^{-1}$ and $17\ \text{J K}^{-1}\,\text{mol}^{-1} \leq \Delta S^\circ \leq 51\ \text{J K}^{-1}\,\text{mol}^{-1}$ or $-26\ \text{kJ mol}^{-1} \leq \Delta H^\circ \leq 36\ \text{kJ mol}^{-1}$ and $59 \leq \Delta S^\circ \leq 249\ \text{J K}^{-1}\,\text{mol}^{-1}$, respectively. The results of these parameters showed that $P2X_1$ receptors are not thermodynamically discriminated and that the binding of agonists and antagonists was both enthalpy and entropy-driven. $P2X_3$ receptors were thermodynamically discriminated and purinergic agonist binding was enthalpy and entropy-driven while antagonist binding was totally entropy-driven. The analysis of such thermodynamic data makes it possible to obtain additional information on the nature of the forces driving the purinergic binding interaction. These data could be interesting in drug discovery programs aimed at development of novel and potent $P2X_1$ and $P2X_3$ purinergic ligands.

* *Corresponding author*. Tel.: +39 0532 291214; fax: +39 0532 291205.
E-mail address: bpa@unife.it (P.A. Borea).

Abbreviations: HEK, human embryonic kidney; [^{3}H]αβmeATP, α,βmethyleneATP; ATP, adenosine 5′ triphosphate; ADP, adenosine 5′ dihosphate; 2meSATP, 2methylSATP; BzATP′benzoylATP; TNP-ATP, 2′-3′-O-(2,4,6-trinitrophenyl)adenosine 5′-triphosphate; PPADS, pyridoxal 5-phosphate 6-azophenyl-2′,4′-disulphonic acid; NF023, 8,8′-[carbonylbis (imino-3,1-phenylene carbonylimino)]bis(1,3,5-naphthalene-trisulfonic acid); NF279, 8,8′-[carbonylbis(imino-4,1-phenylenecarbonyl-imino-4,1-phenylene carbonyl- imino)] bis-1,3,5-naphthalene-trisulphonic acid; A317491, 5-({[3-phenoxybenzyl][(1S)-1,2,3,4-tetrahydro-1-naphthalenyl]amino}carbonyl)-1,2,4-benzene-tricarboxylic acid.

0006-2952/$ – see front matter
doi:10.1016/j.bcp.2007.10.034

1. Introduction

P2 purinergic receptors are divided in two subfamilies: G-protein coupled (P2Y) and ligand-gated ion channels (P2X). In mammalian cells eight P2Y ($P2Y_{1,2,4,6,11,12,13,14}$), seven homomeric P2X ($P2X_{1-7}$) and four heteromeric ($P2X_{2/3}$, $P2X_{1/5}$, $P2X_{2/6}$, $P2X_{4/6}$) receptors have been cloned and characterized pharmacologically [1]. Both of these receptor families are activated by the presence of extracellular adenosine 5′-triphosphate (ATP), an important local regulatory factor under physiological, inflammatory and neuropathic pain conditions [2–4]. Briefly, P2X receptors are abundantly distributed, and functional responses have been reported in neurons, glia, epithelia, endothelia, bone, muscle and hemopoietic tissues [5]. The widespread expression of $P2X_1$ receptors suggests that ATP may contribute in various pathophysiological conditions [6]. $P2X_3$ receptors have been found primarily localized to specific subsets of sensory nociceptor neurones, and there is now much evidence that $P2X_3$ homomeric and $P2X_{2/3}$ heteromeric receptors in sensory pathways are involved in neuropathic and chronic pain [7,8]. Pharmacological methods and manipulations, that can differentiate between $P2X_1$ and $P2X_3$ receptors, could be very useful in the development of $P2X_1$ or $P2X_3$ receptor-specific ligands [9,10]. This is especially important because the rapidly desensitizing kinetics and the agonist and antagonist pharmacology of these two P2X receptors are remarkably similar to each other [1–3]. ATP, and the ATP analogues, BzATP, 2meSATP and αβmeATP show equipotent agonist profiles at $P2X_1$ and $P2X_3$ receptors [11]. Considerable changes in binding affinity of purinergic antagonists are also reported probably due to the little information available with respect to the regions of the receptor involved in antagonist binding [1,2]. More recently, a submicromolar affinity, non-nucleotide antagonist, A 317491, has been described which is more than 100-fold selective for $P2X_3$/$P2X_{2/3}$ receptors over $P2X_1$ receptors in electrophysiological and calcium flux functional assays [12,13]. Radioligand binding techniques have had limited success in differentiating between endogenous or recombinant P2X receptors, probably due to the lack of highly selective and potent ligands [11]. The ATP bioisosteres, [^{3}H]αβmeATP, [^{35}S]ADPβS and [^{35}S]ATPγS have been used in ligand-binding studies of purinergic receptors in various tissues and recombinant expression systems [12,14–17]. In spite of the problems associated with the use of these radioligands, information obtained from specific binding assays has long proved invaluable for screening potential drug candidates, for basic pharmacological characterization of receptor subtypes and for identification of signal transduction pathways. It can be of interest to obtain determinations of drug–receptor binding association (K_A) and dissociation ($1/K_A$ or K_D) constants over a range of temperatures, in contrast to the single-point temperature assays, which add significant information on the molecular mechanisms involved in the drug–receptor interaction [18]. Determination of K_A or K_D values makes it possible to calculate the standard free energy $\Delta G^\circ = -RT\ln K_A = RT\ln K_D$ ($T = 298.15$ K), but not its two components, the equilibrium standard enthalpy (ΔH°) and entropy (ΔS°) as defined by the Gibbs equation $\Delta G^\circ = \Delta H^\circ - T\Delta S^\circ$. As a consequence, van't Hoff plot analysis was performed to obtain K_D values over a range of temperatures and to obtain the thermodynamic terms of this equation. From such analysis, it is generally proposed that standard enthalpy is a quantitative indicator of the changes in intermolecular bond energies, such as hydrogen bonding and van der Waals interactions, occurring during the binding. In addition standard entropy can be considered an indicator of the rearrangements undergone by the solvent, normally water molecules, during the same process [18]. In the last few years it has been shown that the ΔH° and ΔS° values of drug interaction with a defined receptor can often give a simple *in vitro* way to discriminate agonists from antagonists suggesting the manner in which the drug interferes with the signal transduction pathways.

Such "thermodynamic discrimination" reveals that the binding of agonists may be entropy-driven and that the antagonists are enthalpy-driven, or *vice versa*. At the present fourteen receptor systems have been extensively studied so far from thermodynamic point of view: eleven of these show the agonist-antagonist discrimination and three are not discriminated [18–22]. In particular, all the ligand-gated ion channel receptors, *i.e.* glycine, GABA, $5HT_3$ and neuronal nicotinic receptors have been reported to discriminate *in vitro* the effect of their agonists and antagonists [23–25]. Analysis of thermodynamic data of drug–receptor interactions appears to be an effective tool in the study of the role, at the molecular level, played during the binding of the ligands [18–20].

From this background, the aim of this study was to determine the thermodynamic parameters of typical agonists and antagonists in HEK 293 cells transfected with human $P2X_1$ and $P2X_3$ receptors by using [^{3}H]αβmeATP radioligand binding assays and van't Hoff analysis in order to gain further insight into possible differences in pharmacological properties between these two therapeutically important P2X receptor subtypes. Striking differences in thermodynamic properties of these receptor subtypes were found. In particular, $P2X_1$ receptors are not thermodynamically discriminated with the enthalpy/entropy-driven binding of both agonists and antagonists while $P2X_3$ receptors are thermodynamically discriminated with enthalpy/entropy-driven agonist binding but solely entropy-driven antagonist binding. This research could provide information in the development of novel and potent $P2X_1$ and $P2X_3$ purinergic ligands.

2. Materials and methods

2.1. Materials

[^{3}H]αβmeATP (specific activity 15.0 Ci mmol^{-1}) was obtained from NEN-Perkin Elmer Life and Analytical Sciences (USA). ATP, ADP, αβmeATP, BzATP, TNP-ATP, suramin, NF023, PPADS, A 317491 and apyrase were obtained from Sigma–Aldrich Advanced Sciences (Milan, Italy). NF279 and 2meSATP were obtained from Tocris Cookson Ltd. (Bristol, UK). All other reagents were of analytical grade and obtained from commercial sources.

2.2. Cell culture and membrane preparation

HEK293-h$P2X_1$ and HEK293-h$P2X_3$ cells were kindly provided by Prof. A. Surprenant (Institute of Molecular Physiology,

University of Sheffield, Sheffield, England, UK). Methods of maintenance of HEK293 cells and their stable transfection with $hP2X_1$ and $hP2X_3$ receptors cDNA have been described previously [26]. Briefly, the cells were grown adherently and maintained in Dulbecco's Modified Eagle's Medium with nutrient mixture F12 (DMEM/F12), containing 10% fetal calf serum, penicillin (100 U mL^{-1}), streptomycin (100 μg mL^{-1}) and Geneticin (G418, 0.2 mg mL^{-1}) at 37 °C in 5% CO_2/95% air. Cells were split two or three times weekly at a ratio of 1:5. For membrane preparation, the culture medium was removed and the cell suspension was washed with PBS and scraped in ice-cold hypotonic buffer (5 mM Tris–HCl, 2 mM EDTA, pH 7.4). The cell suspension was homogenized with Polytron (Kinematica, Switzerland) at a setting of 6 for 40 s and the homogenate was spun for 30 min at 100,000 × *g* and frozen at −80 °C until binding experiments.

2.3. *Effect of various factors on purinergic receptor binding assays*

The effect of pH at the different values (6.0, 7.0, 7.4, 8.0, 9.0) on the [^{3}H]αβmeATP binding at the 3 nM concentration was evaluated and obtained incubating in 50 mM Tris–HCl the HEK-293 membranes containing $hP2X_1$ or $hP2X_3$ purinergic receptors.

The effect of different concentrations of Ca^{2+} (from 0 to 10 mM) and Mg^{2+} (from 0 to 10 mM) was also investigated by using 3 nM of [^{3}H]αβmeATP as radioligand in 50 mM Tris–HCl pH 7.4 and HEK-293 membranes containing $hP2X_1$ or $hP2X_3$ purinergic receptors.

The effect of Apyrase (1 U/ml for 30 min at 37 °C) was evaluated incubating the $hP2X_1$ or $hP2X_3$ membranes in 50 mM Tris–HCl pH 7.4, 4 mM $CaCl_2$ and 3 nM of [^{3}H]αβmeATP as radioligand.

Non-specific binding was determined in the presence of 10 μM αβmeATP [27]. After the incubation time (40 min at 5 °C) bound and free radioactivity were separated by rapid filtration through Whatman GF/B glass-fiber filters using a Brandel instrument. The filter bound radioactivity was counted on a Scintillation Counter Tri Carb Packard 2500 TR (efficiency 57%).

2.4. *Kinetics of [^{3}H]αβmeATP binding*

Kinetic studies of 3 nM [^{3}H]αβmeATP were performed by incubating membranes in 50 mM Tris–HCl, 4 mM $CaCl_2$, pH 7.4 obtained as described above in a thermostatic bath at 5 °C. For the measurement of the association rate of human $P2X_1$ receptors, the reaction was terminated at different times (from 1 to 80 min) by rapid filtration under vacuum, followed by washing four times with ice cold buffer. Similarly, for human $P2X_3$ receptors the reaction was terminated from 10 s to 30 min by rapid filtration. For the measurement of the dissociation rate, the samples were incubated at 5 °C for 40 min and then 10 μM αβmeATP was added to the mixture. The reaction was terminated for $P2X_1$ receptors from 1 to 40 min and for $P2X_3$ receptors from 30 s to 40 min.

2.5. *Saturation and competition binding experiments*

Saturation and competition binding assays were performed on HEK293-$hP2X_1$ and HEK293-$hP2X_3$ membranes at 5, 10, 15, 20, 25

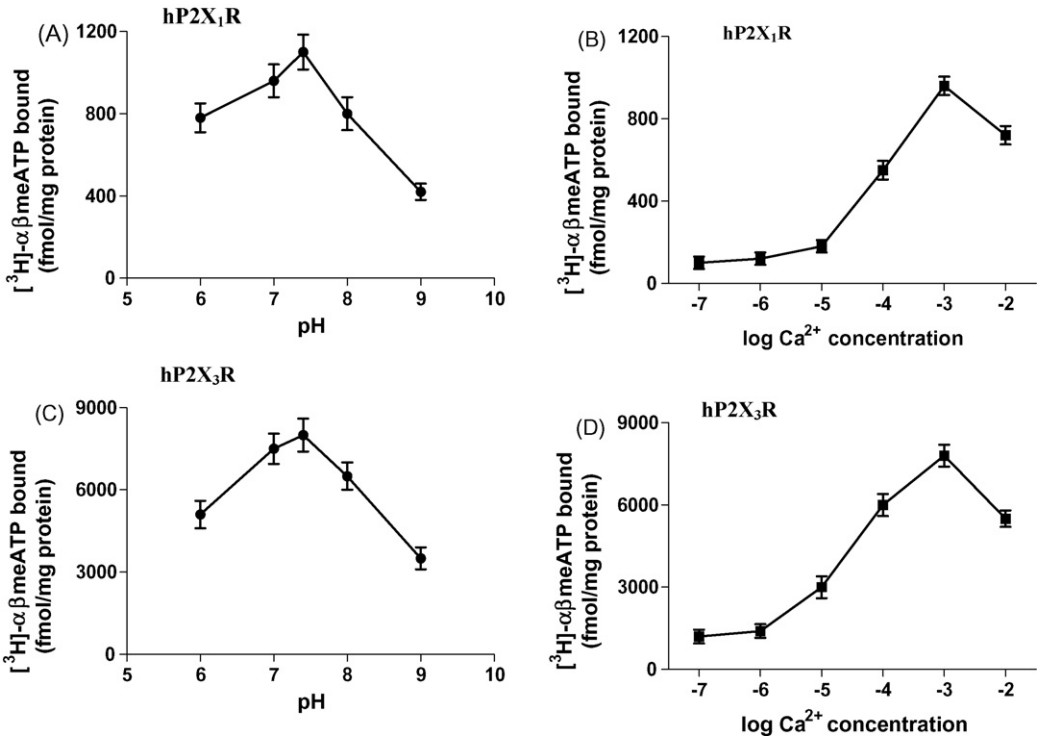

Fig. 1 – Effect of pH on the [^{3}H]αβmeATP binding in HEK293-$hP2X_1$ and HEK293-$hP2X_3$ membranes (A, C). Effect of Ca^{2+} on [^{3}H]αβmeATP binding in HEK293-$hP2X_1$ and HEK293-$hP2X_3$ membranes (B, D). Data represent mean ± S.E.M. of three independent experiments each performed in duplicate.

and 30 °C, in a thermostatic bath assuring a temperature of ±0.1 °C. Analogous experiments in HEK293 wild type and in HEK293 transfected with the vector alone were executed. Saturation binding experiments of [^{3}H]αβmeATP (0.1–50 nM) to the membranes previously obtained were performed in 50 mM Tris–HCl, 4 mM $CaCl_2$ pH 7.4 for an incubation time ranged from 40 min at 5 °C to 90 min at 30 °C according to the results of previous time-course experiments. Competition experiments of 3 nM [^{3}H]αβmeATP were performed in the same buffer described above and at least 8–10 different concentrations of $P2X_1$ and $P2X_3$ agonists or antagonists studied. Non-specific binding was determined in the presence of 10 μM αβmeATP [27]. Bound and free radioactivity were separated by rapid filtration through Whatman GF/B glass-fiber filters using a Brandel instrument. The filter bound radioactivity was counted on a Scintillation Counter Tri Carb Packard 2500 TR (efficiency 57%). The affinity values expressed as K_D or K_i were used in the thermodynamic parameter determination.

2.6. Thermodynamic data determination

For a generic binding equilibrium L + R = LR (L = ligand, R = receptor) the affinity association constant $K_A = 1/K_D$ is directly related to the standard free energy ΔG° ($\Delta G^\circ = -RT\ln K_A$) which can be separated in its enthalpic and entropic contributions according to the Gibbs equation: $\Delta G^\circ = \Delta H^\circ - T\Delta S^\circ$. The standard free energy was calculated as $\Delta G^\circ = -RT\ln K_A$ at 298.15 K, the standard enthalpy, ΔH°, from the van't Hoff plot $\ln K_A$ versus (1/T) (the slope of which is $-\Delta H^\circ/R$) and the standard entropy as $\Delta S^\circ = (\Delta H^\circ - \Delta G^\circ)/T$ with T = 298.15 K and R = 8.314 J/K mol [18,25,28].

2.7. Data analysis

Kinetic, saturation and competition binding experiments were analyzed with the program ligand [29] which

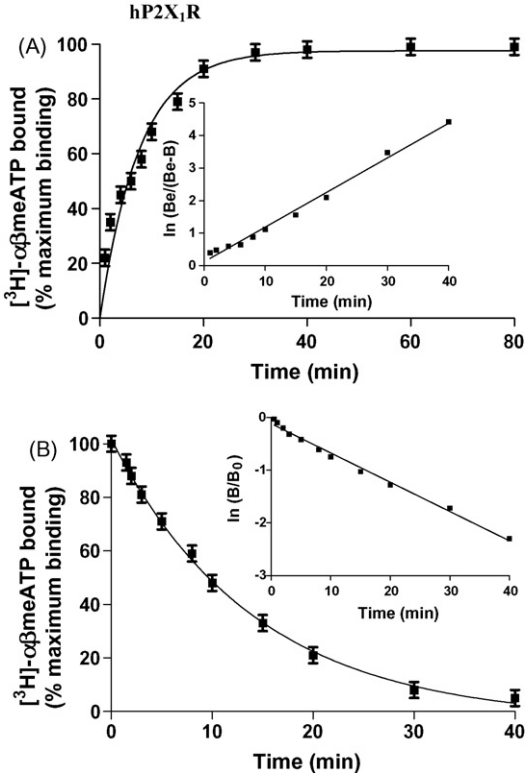

Fig. 2 – Kinetics of 3 nM [^{3}H]αβmeATP binding to HEK293-hP2X$_1$ membranes with association curves relative to three independent experiments (A). In the inset first-order plots of [^{3}H]αβmeATP binding. B_e represents the amount of [^{3}H]αβmeATP bound at equilibrium, and B represents the amount of [^{3}H]αβmeATP bound at each time, B_0 represents the amount of [^{3}H]αβmeATP bound at time zero. Association rate constant was: K_{+1} = 0.017 ± 0.002 min^{-1} nM^{-1}. Kinetics of [^{3}H]αβmeATP binding to human purinergic P2X$_1$ receptors with dissociation curves relative of three independent experiments (B). In the inset, first order plots of [^{3}H]αβmeATP binding. Dissociation rate constant was: K_{-1} = 0.056 ± 0.003 min^{-1}.

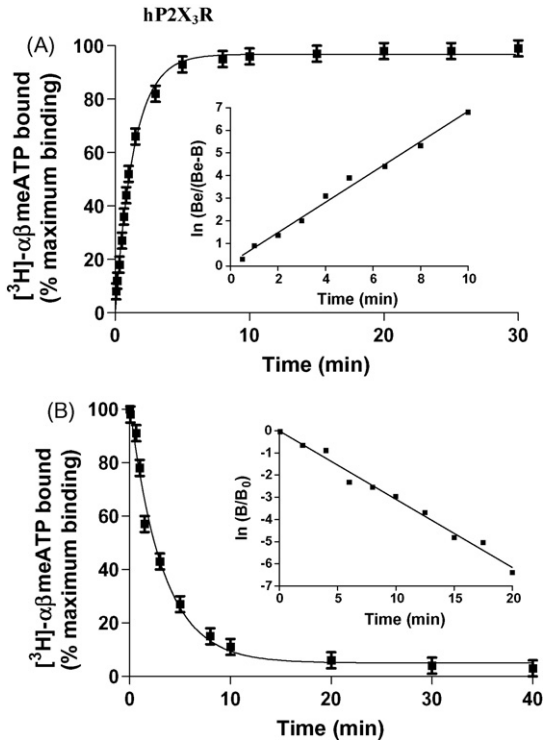

Fig. 3 – Kinetics of 3 nM [^{3}H]αβmeATP binding to HEK293-hP2X$_3$ membranes with association curves relative of three independent experiments (A). In the inset first-order plots of [^{3}H]αβmeATP binding. B_e represents the amount of [^{3}H]αβmeATP bound at equilibrium, B represents the amount of [^{3}H]αβmeATP bound at each time, B_0 represents the amount of [^{3}H]αβmeATP bound at time zero. Association rate constant was: K_{+1} = 0.133 ± 0.014 min^{-1} nM^{-1}. Kinetics of [^{3}H]αβmeATP binding to human purinergic P2X$_1$ receptors with dissociation curves relative of three independent experiments (B). In the inset, first-order plots of [^{3}H]αβmeATP binding. Dissociation rate constant was: K_{-1} = 0.313 ± 0.027 min^{-1}.

Table 1 – Binding parameters of HEK293-hP2X$_1$ and HEK293-hP2X$_3$ membranes (A) and thermodynamic parameters for the binding equilibrium of [^{3}H]αβmeATP in the same substrates (B)

(A)

[^{3}H]αβme ATP binding	5 °C (278 K)	10 °C (283 K)	15 °C (288 K)	20 °C (293 K)	25 °C (298 K)	30 °C (303 K)
HEK293-hP2X$_1$ K_D (nM)	3.2 ± 0.3	4.1 ± 0.4	4.8 ± 0.4	6.4 ± 0.6	8.1 ± 0.7	11.1 ± 1.1
B_{max} (fmol/mg protein)	3120 ± 290	3200 ± 310	3300 ± 320	3400 ± 330	3050 ± 315	3500 ± 325
HEK293-hP2X$_3$ K_D (nM)	2.6 ± 0.3	3.5 ± 0.4	4.0 ± 0.4	4.9 ± 0.5	6.2 ± 0.6	7.5 ± 0.7
B_{max} (fmol/mg protein)	18800 ± 1600	18900 ± 1650	19000 ± 1700	19200 ± 1750	18500 ± 1520	19500 ± 1800

(B)

Cell lines	ΔG° (kJ mol^{-1})	ΔH° (kJ mol^{-1})	ΔS° (J mol^{-1} K^{-1})
HEK293-hP2X$_1$	−46.0 ± 0.2	−32 ± 3	46 ± 3
HEK293-hP2X$_3$	−46.7 ± 0.2	−28 ± 2	64 ± 6

ΔG°, ΔH° and ΔS° values are given at 298 K.
Dissociation constants (K_D, nM) and B_{max} values (fmol/mg protein) are referred to the binding of [^{3}H]αβmeATP to hP2X$_1$ and hP2X$_3$ purinergic receptors. Data are mean ± S.E.M. from at least four independent experiments performed in duplicate.

performs weighted non-linear least-squares curve fitting program.

The protein concentration was determined according to a Bio-Rad method with bovine albumin as reference standard [30]. All experimental data are reported as mean ± standard error of the mean (S.E.M.) of three or four independent experiments performed in duplicate.

3. Results

3.1. *Effect of various factors on purinergic receptor binding assays*

Preliminary assays were performed to determine the experimental conditions for the evaluation of specific [^{3}H]αβmeATP

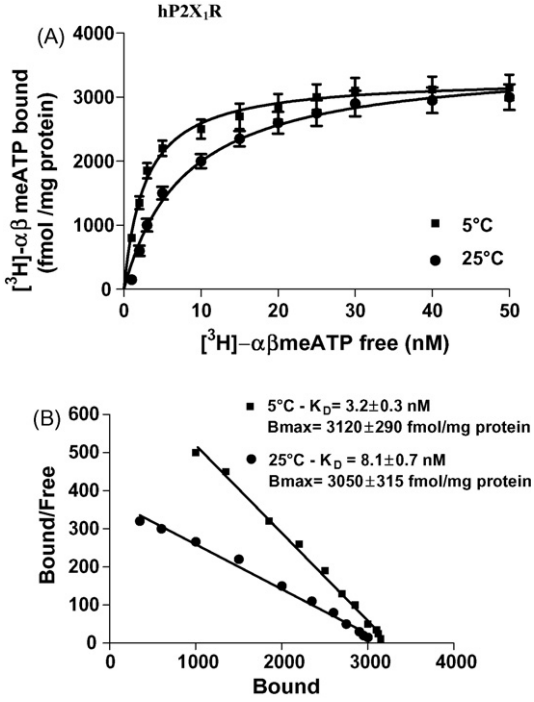

Fig. 4 – Saturation curves of [^{3}H]αβmeATP to HEK293-hP2X$_1$ cells at 5 and 25 °C (A). The linearity of the corresponding Scatchard plot (B) is indicative of the presence of a single class of high affinity binding site at the temperatures investigated. Values are the means and the vertical lines are the S.E.M. of four independent experiments each performed in duplicate. The Scatchard plot of the same data is shown.

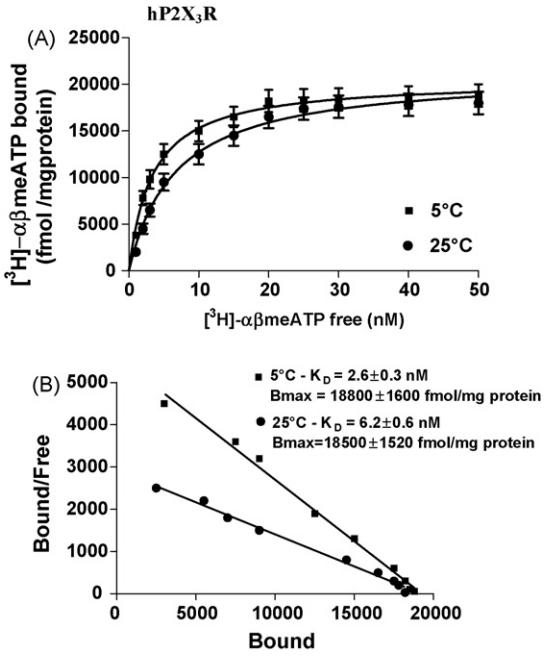

Fig. 5 – Saturation curves of [^{3}H]αβmeATP to HEK293-hP2X$_3$ cells at 5 and 25 °C (A). The linearity of the corresponding Scatchard plot (B) is indicative of the presence of a single class of high affinity binding site at the temperatures investigated. Values are the means and the vertical lines are the S.E.M. of four independent experiments each performed in duplicate. The Scatchard plot of the same data is shown.

binding. The incubation of the HEK293-hP2X$_1$ and HEK293-hP2X$_3$ membranes with apyrase (1 U/ml) with the aim to eliminate extracellular ATP and minimize receptor desensitization during binding experiments produced no differences in the percentage of specific binding (HEK293-hP2X$_1$ = 85 ± 8% and 88 ± 9% or HEK293-hP2X$_3$ = 89 ± 9% and 92 ± 10%, respectively).

The effect of pH values (from 6 to 9) on the [^{3}H]αβmeATP binding reveals that the optimal pH value for the binding experiments was around 7.4 in both cell lines examined (Fig. 1A and C). The specific binding of [^{3}H]αβmeATP to HEK293-hP2X$_1$ (Fig. 1B) and HEK293-hP2X$_3$ (Fig. 1D) membranes increased of 8- and 6-fold, respectively with the raise of the Ca^{2+} concentration from 1 μM to 1 mM. On the contrary, further increasing in the calcium concentration from 1 to 10 mM led to a decline of specific [^{3}H]αβmeATP binding. The addition of Mg^{2+} (from 1 to 10 mM) in the same experimental conditions resulted in a strong reduction (80%, $n = 3$) of the binding suggesting that the [^{3}H]αβmeATP binding was regulated in an opposite way by physiological concentrations of Ca^{2+} and Mg^{2+}, respectively.

3.2. *Kinetic binding assays to human P2X$_1$ and P2X$_3$ purinergic receptors*

Kinetic behavior of [^{3}H]αβmeATP binding was studied at 5 °C in HEK293-hP2X$_1$ (Fig. 2) and HEK293-hP2X$_3$ (Fig. 3) membranes. Figs. 2A and 3A show that [^{3}H]αβmeATP binding reached equilibrium after approximately 20 and 5 min, respectively and was stable for at least 90 min. [^{3}H]αβmeATP binding was rapidly reversed by the addition of 10 μM αβmeATP as shown in Figs. 2B and 3B. Association and dissociation curves in HEK293-hP2X$_1$ and HEK293-hP2X$_3$ membranes were fitted to a one component model significantly better than to a two component model ($P < 0.05$). The rate constants were: $k_{obs} = 0.106 \pm 0.012\ min^{-1}$ and $0.712 \pm 0.010\ min^{-1}$, respectively. The k_{+1} values were $0.017 \pm 0.002\ min^{-1}\ nM^{-1}$ and $0.133 \pm 0.014\ min^{-1}\ nM^{-1}$, respectively. The apparent equilibrium dissociation constant (K_D) was estimated to be 3.29 nM and 2.35 nM, respectively.

3.3. *Saturation binding assays to human P2X$_1$ and P2X$_3$ purinergic receptors*

Saturation binding experiments in HEK 293 cells were performed to better characterize human P2X$_1$ and P2X$_3$ purinergic receptors and evaluate affinity (K_D) and receptor density (B_{max}) values (Table 1). These binding parameters were determined at various temperatures by using [^{3}H]αβmeATP as radioligand at different concentrations. In both purinergic receptors examined the K_D values change with temperature and B_{max} values appear to be largely independent of it. Figs. 4 and 5 illustrate saturation binding curves and Scatchard plot relative to human P2X$_1$ and P2X$_3$ purinergic receptors, respectively. Scatchard plots were linear at all temperatures investigated and computer analysis of the data failed to show a significantly better fit to a two site than to a one site binding model, indicating that only one class of high affinity binding site was present under our experimental conditions.

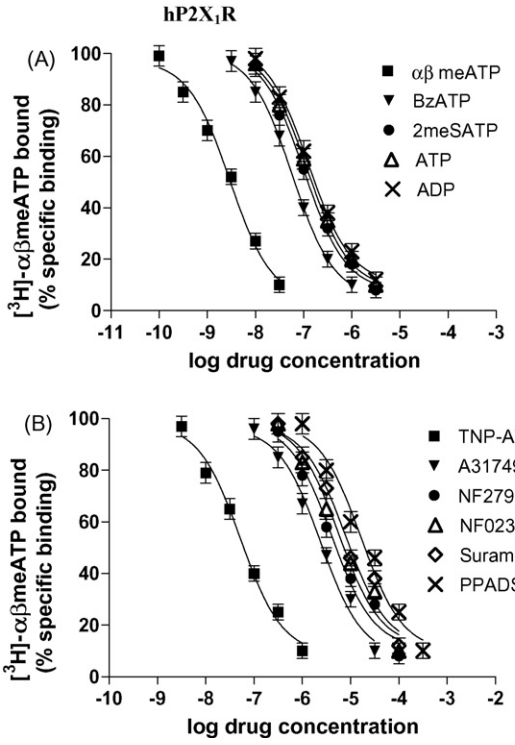

Fig. 6 – Competition curves of specific 3 nM [^{3}H]αβmeATP binding to HEK293-hP2X$_1$ by purinergic agonists (A) and antagonists (B). Curves represent the means ± S.E.M. of four independent experiments each performed in duplicate.

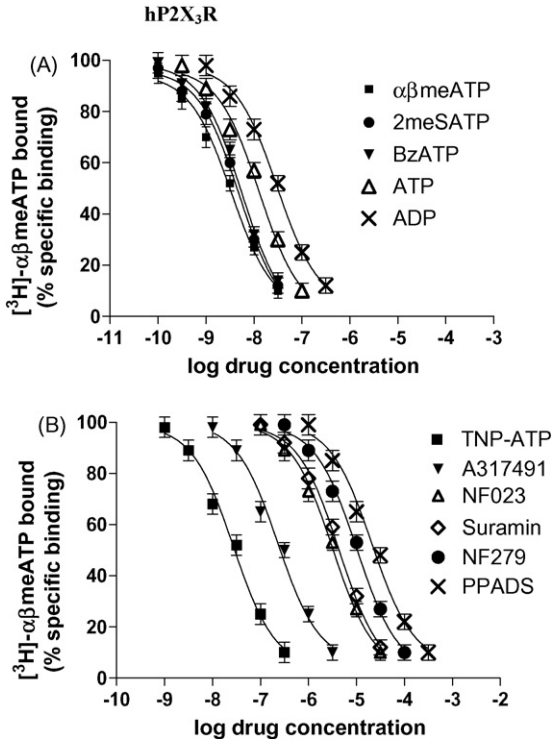

Fig. 7 – Competition curves of specific 3 nM [^{3}H]αβmeATP binding to HEK293-hP2X$_3$ by purinergic agonists (A) and antagonists (B). Curves represent the means ± S.E.M. of four independent experiments each performed in duplicate.

Saturation binding experiments performed employing HEK 293 wild type and HEK 293 transfected with the vector alone failed to show significant values of specific binding ($n = 4$ experiments, % of specific binding = $2 \pm 1\%$ and $3 \pm 1\%$, respectively) suggesting that the $P2X_1$ and $P2X_3$ transfection is essential to the presence of specific binding.

3.4. *Competition binding assays to human $P2X_1$ and $P2X_3$ purinergic receptors*

Figs. 6 and 7 show the dose response curves of [^{3}H]αβmeATP binding in HEK293-h$P2X_1$ and HEK293-h$P2X_3$ membranes by using typical agonists and antagonists. The order of potency in [^{3}H]αβmeATP displacement assays for purinergic agonists in HEK293-h$P2X_1$ was as follows: αβmeATP > BzATP > 2meSATP > ATP > ADP. A similar order of potency was also obtained in HEK293-h$P2X_3$ even if the affinity values were much higher than in HEK293-h$P2X_1$ membranes. The order of potency of antagonists in HEK293-h$P2X_1$ was similar to those obtained in HEK293-h$P2X_3$ as follows: TNP-ATP > A 317491 > NF 279 > NF 023 > Suramin > PPADS and TNP-ATP > A 317491 > NF 023 > Suramin > NF 279 > PPADS, respectively.

3.5. *Thermodynamic analysis to human $P2X_1$ and $P2X_3$ purinergic receptors*

The van't Hoff plots show that the effect of temperature on the equilibrium binding association constants, K_A appears to be essentially linear in the range 4-30 °C for purinergic ligands examined to human $P2X_1$ and $P2X_3$ purinergic receptors (Figs. 8 and 9). Slopes of van't Hoff plots are positive for agonists and antagonists of $P2X_1$ purinergic receptors showing that the affinities decrease with the increase of the temperature (Table 2A). On the contrary the slopes of the van't Hoff plots regarding $P2X_3$ purinergic receptors are positive for agonists whose affinities decrease with the increase of the temperature and negative for antagonists whose affinities are improved by an increase in temperature (Table 2B). Final thermodynamic parameters (expressed as mean values ±standard error of four independent experiments) calculated for the binding equilibria of the different compounds investigated are reported in Table 3.

In $P2X_1$ purinergic receptors ΔG° values range from −46.0 to −37.4 kJ mol^{-1} for agonists and from −30.1 to −25.5 kJ mol^{-1} for antagonists. In $P2X_3$ purinergic receptors ΔG° values range from −46.2 to −41.0 kJ mol^{-1} for agonists and from −39.8 to −29.3 kJ mol^{-1} for antagonists. Equilibrium standard enthalpy ΔH° and entropy ΔS° values show similar values for agonists and antagonists examined suggesting that $P2X_1$ purinergic receptors are not thermodynamically discriminated. On the contrary, the analysis of thermodynamic parameters of $P2X_3$ purinergic receptors shows that the binding for agonists is always enthalpy- and entropy-driven (ΔH° values ranging from −26 to −18 kJ mol^{-1} and ΔS° values from 59 to 68 JK^{-1} mol^{-1}) while for antagonists it is totally entropy-driven (ΔH° values ranging from 14 to 36 kJ mol^{-1} and ΔS° values from

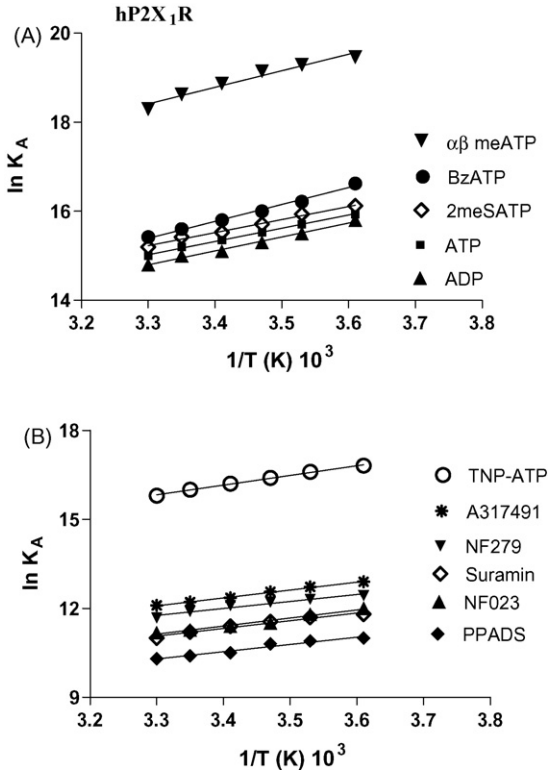

Fig. 8 – van't Hoff plots showing the effect of temperature on the equilibrium binding association constants, K_A, for $P2X_1$ purinergic agonists (A) and antagonists (B) studied. All plots are essentially liner ($r \geq 0.93$) in the temperature range of 5–30 °C.

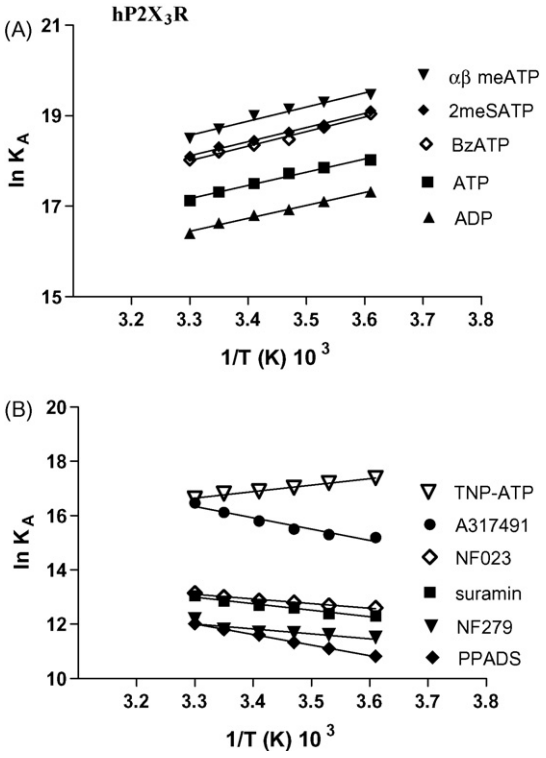

Fig. 9 – van't Hoff plots showing the effect of temperature on the equilibrium binding association constants, K_A, for $P2X_3$ purinergic agonists (A) and antagonists (B) studied. All plots are essentially linear ($r \geq 0.95$) in the temperature range of 5–30 °C.

Table 2 – Affinities, expressed as K_i values (nM) of selected purinergic compounds to human $P2X_1$ (A) and $P2X_3$ (B) receptors expressed in HEK293 cells

(A)

Ligand	5 °C (278 K)	10 °C (283 K)	15 °C (288 K)	20 °C (293 K)	25 °C (298 K)	30 °C (303 K)
Purinergic agonists, K_i (nM)						
ATP	120 ± 10	150 ± 14	180 ± 15	215 ± 20	250 ± 24	306 ± 28
ADP	125 ± 11	155 ± 13	200 ± 16	227 ± 18	245 ± 22	316 ± 30
αβmeATP	3.5 ± 0.3	4.2 ± 0.4	4.8 ± 0.5	6.4 ± 0.6	8.1 ± 0.7	11.4 ± 1.1
2meSATP	100 ± 10	120 ± 11	150 ± 12	180 ± 15	200 ± 18	250 ± 22
BzATP	60 ± 6	90 ± 9	113 ± 10	137 ± 12	168 ± 18	200 ± 16
Purinergic antagonists, K_i (nM)						
Suramin	7500 ± 650	8300 ± 730	9600 ± 850	11200 ± 950	13700 ± 1100	16700 ± 1200
NF023	6140 ± 500	7500 ± 600	10000 ± 970	11200 ± 1050	12800 ± 1080	14000 ± 1270
TNP-ATP	50 ± 4	60 ± 5	75 ± 7	92 ± 8	113 ± 10	137 ± 15
PPADS	16700 ± 1500	18500 ± 1700	20400 ± 2000	27500 ± 2400	30400 ± 2800	33600 ± 3120
A317491	2500 ± 220	3000 ± 210	3500 ± 250	4300 ± 300	5000 ± 420	5600 ± 510
NF279	4000 ± 300	4500 ± 350	5000 ± 380	5600 ± 460	6800 ± 610	8500 ± 720

(B)

Ligand	5 °C (278 K)	10 °C (283 K)	15 °C (288 K)	20 °C (293 K)	25 °C (298 K)	30 °C (303 K)
Purinergic agonists, K_i (nM)						
ATP	15 ± 2	18 ± 2	20 ± 2	25 ± 2	30 ± 3	37 ± 4
ADP	30 ± 3	37 ± 3	45 ± 4	50 ± 5	60 ± 5	75 ± 6
αβmeATP	2.9 ± 0.3	4.1 ± 0.4	4.6 ± 0.5	5.3 ± 0.5	7.6 ± 0.6	9.2 ± 0.8
2meSATP	5.1 ± 0.4	6.8 ± 0.5	8.2 ± 0.7	9.7 ± 0.8	11.2 ± 1.0	13.8 ± 1.2
BzATP	5.4 ± 0.4	7.2 ± 0.5	9.4 ± 0.7	10.7 ± 0.9	12.5 ± 1.1	14.9 ± 1.3
Purinergic antagonists, K_i (nM)						
Suramin	4000 ± 380	3730 ± 350	3100 ± 280	2800 ± 245	2500 ± 240	2100 ± 180
NF023	3500 ± 320	3200 ± 300	3000 ± 260	2700 ± 252	2300 ± 210	2000 ± 195
TNP-ATP	28 ± 3	34 ± 3	40 ± 4	46 ± 4	50 ± 5	60 ± 5
PPADS	20000 ± 1850	15000 ± 1200	12000 ± 1100	9170 ± 840	7500 ± 720	6000 ± 510
A317491	250 ± 22	226 ± 20	185 ± 15	137 ± 12	100 ± 9	70 ± 6
NF279	10000 ± 920	9170 ± 810	8290 ± 780	7500 ± 740	6790 ± 630	5560 ± 450

Data are mean ± S.E.M. of four independent experiments performed in duplicate. Inhibition binding experiments were performed as described in Section 2. K_i values represent the concentration of drug able to displace 50% of the radioligand.

149 to 249 $JK^{-1}\,mol^{-1}$). Therefore, agonists and antagonists at $P2X_3$ purinergic receptors are thermodynamically discriminated. Interestingly, the compound TNP-ATP, reported to be from a functional point of view as a purinergic antagonist [13], shows a typical agonist behavior with an affinity value and thermodynamic parameters strictly similar to those obtained for the other purinergic agonists. Fig. 10 summarizes the results in the form $-T\Delta S^\circ$ versus ΔH° scatter plot (T = 298.15 K) showing that for human $P2X_1$ receptors the points are present in the region that characterizes the enthalpy and entropy-driven binding without a thermodynamically discrimination. On the contrary, in human $P2X_3$ purinergic receptors antagonists are clustered in the endothermic region ($14\ kJ\,mol^{-1} \leq \Delta H^\circ \leq 36\ kJ\,mol^{-1}$) with large positive entropy values ($-74.20\ kJ\,mol^{-1} \leq -T\Delta S^\circ \leq -44.40\ kJ\,mol^{-1}$) revealing that their binding is totally entropy-driven. Agonist binding is enthalpy and entropy-driven ($-26\ kJ\,mol^{-1} \leq \Delta H^\circ \leq -18\ kJ\,mol^{-1}$ and $-21.75 \leq -T\Delta S^\circ \leq -17.58\ kJ\,mol^{-1}$).

4. Discussion

Thermodynamic parameters have been collected for a remarkable number of ligands at $P2X_1$ and $P2X_3$ receptors, including full, partial and inverse agonists or antagonists [18]. The information provided by these data could be useful from a pharmacological point of view to discover new thermodynamic relationships related to drug–receptor interactions and their molecular mechanisms [31–33]. In the last few years, it has been reported that equilibrium standard enthalpy (ΔH°) and entropy (ΔS°) values of drug interaction with a defined receptor can often give a simple "*in vitro*" way to discriminate the capability of the drug to interfere with the signal transduction pathways [18–22,34]. This phenomenon, called "thermodynamic discrimination" has been evaluated for various membrane and cytoplasmatic/nuclear receptors. Six G-protein coupled receptors such as β-adrenergic, D_2 dopamine, $5HT_{1A}$ serotonin and A_1, A_{2A} and A_3 adenosine subtypes were studied and four out of six of these were thermodynamically discriminated [18,20,21]. In addition four ligand-gated ion channel receptors such as glycine, $GABA_A$, $5HT_3$ serotonin and nicotinic membrane receptors were analyzed and all resulted discriminated from a thermodynamic point of view [23–25]. Finally, the cytoplasmatic receptor for glucocorticoid hormones and three cytoplasmatic steroid/nuclear estrogen, progesterone and androgen receptors were investigated and three of these were discriminated [22]. All these data suggest an intercorrelation between specific binding and the variation

Table 3 – Thermodynamic parameters for the binding equilibrium of [^{3}H]αβmeATP to human P2X$_1$ (A) and P2X$_3$ (B) purinergic receptors expressed in HEK293 cells

(A)

Ligand	ΔG° (kJ mol^{-1})	ΔH° (kJ mol^{-1})	ΔS° (J mol^{-1} K^{-1})
Purinergic agonists			
ATP	−37.4 ± 0.1	−25 ± 3	43 ± 3
ADP	−37.6 ± 0.1	−24 ± 2	47 ± 3
αβmeATP	−46.0 ± 0.2	−31 ± 3	51 ± 4
2meSATP	−37.8 ± 0.1	−24 ± 1	46 ± 3
BzATP	−38.4 ± 0.1	−23 ± 2	50 ± 4
Purinergic antagonists			
Suramin	−27.8 ± 0.1	−21 ± 2	21 ± 3
NF023	−27.6 ± 0.1	−22 ± 2	20 ± 2
TNP-ATP	−39.3 ± 0.2	−27 ± 3	41 ± 4
PPADS	−25.5 ± 0.1	−20 ± 2	17 ± 1
A317491	−30.1 ± 0.2	−22 ± 3	27 ± 2
NF279	−29.3 ± 0.1	−19 ± 1	34 ± 2

(B)

Ligand	ΔG° (kJ mol^{-1})	ΔH° (kJ mol^{-1})	ΔS° (J mol^{-1} K^{-1})
Purinergic agonists			
ATP	−42.7 ± 0.1	−24 ± 1	62 ± 5
ADP	−41.0 ± 0.1	−24 ± 2	59 ± 4
αβmeATP	−46.2 ± 0.2	−26 ± 3	68 ± 5
2meSATP	−45.1 ± 0.2	−26 ± 2	65 ± 5
BzATP	−44.9 ± 0.1	−18 ± 2	64 ± 4
Purinergic antagonists			
Suramin	−31.9 ± 0.1	18 ± 2	168 ± 8
NF023	−32.0 ± 0.1	14 ± 1	153 ± 8
TNP-ATP	−41.4 ± 0.2	−20 ± 2	73 ± 6
PPADS	−29.3 ± 0.1	36 ± 3	218 ± 9
A317491	−39.8 ± 0.2	35 ± 3	249 ± 9
NF279	−29.5 ± 0.1	15 ± 2	149 ± 7

Equilibrium ΔG°, ΔH° and ΔS° values are given at 298 K.

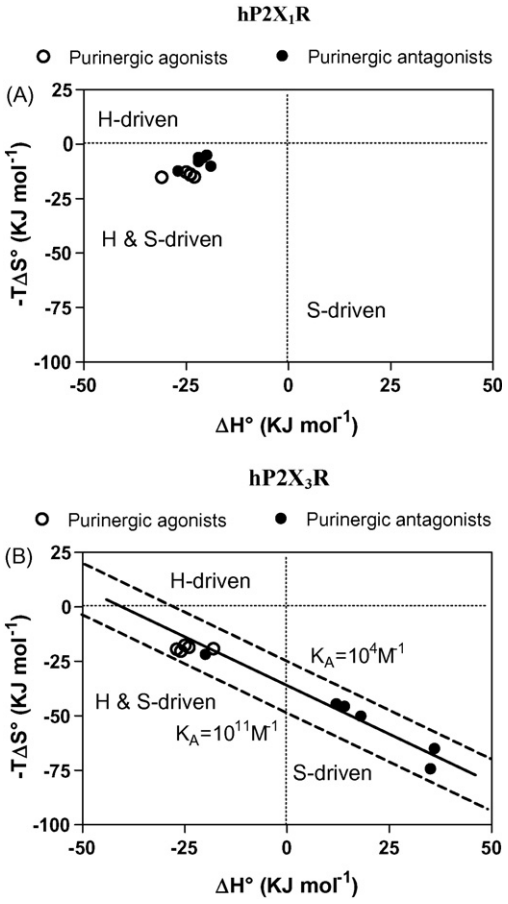

Fig. 10 – Scatter plot showing $-T\Delta S^\circ$ versus ΔH° values for the purinergic ligands studied in HEK293-hP2X$_1$ (A) and HEK293-hP2X$_3$ (B). Full and open symbols indicate antagonists and agonists, respectively. All points lie on a same regression line for compounds of Table 3. The linear regression of the points ($R = 0.985$, $P < 0.0001$) evidences a typical enthalpy–entropy compensation phenomenon.

of water molecules present to receptor surfaces. In addition, based on the thermodynamic compensation a general model of drug–receptor interaction has been proposed. In this model the solvent molecules do not modify the intrinsic values of the affinity constant (K_A) of the drug–receptor interaction because the standard free energy for solvent reorganization can be near to zero and the values of binding parameters are due to specific features of the ligand and receptor in the binding process and not by the solvent [32]. On the other hand, ΔH° and $-T\Delta S^\circ$ values are related to the rearrangements occurring during the binding, in the solvent–drug and solvent–receptor interfaces [32]. It seems reasonable to assume that solvent effects might be responsible for the *in vitro* thermodynamic discrimination between agonists and antagonists.

From this background, one of the most significant results of this paper is the presence of the linearity of van't Hoff plots for P2X purinergic receptors similarly to what verified for other membrane receptors showing that ΔH° and ΔS° values are independent of temperature and obtained by linear van't Hoff plots [18–22]. van't Hoff plots turn out to be linear for all compounds considered implying that the value of ΔH° is not significantly affected by temperature variation in the range investigated.

The second result concerns the interdependence of ΔH° and $-T\Delta S^\circ$ values for the P2X$_3$ purinergic receptors where all the experimental points appear to be arranged along a same diagonal line according to the equation: $-T\Delta S^\circ$ (kJ mol^{-1} at 278 K) = −37.8 (±2) − 0.80 (±0.05) ΔH° (kJ mol^{-1}) ($n = 11$, $r = 0.985$, $P < 0.0001$). This equation is of the form $\Delta H^\circ = \beta\Delta S^\circ$ which is expected for a case of enthalpy–entropy compensation with a compensation temperature of 278 K [18–22]. The enthalpy–entropy compensation phenomenon has been attributed for drug–receptor interactions to the solvent reorganization [32]. While ΔG° values are most probably determined by the features of the ligand–receptor binding process, ΔH° and $-T\Delta S^\circ$ values appear strongly affected by the rearrangements occurring in the solvent [35]. As it can be seen from the data plotted in Fig. 10, all experimental points are arranged on the same diagonal band encompassed between the two dashed lines which represent the *loci* of points defined by the limiting K_D values of 100 μM and 10 pM. This band is the expression of the enthalpy–entropy compensation phenomenon probably due to drug–receptor interactions and to the solvent reorganization that accompanies the receptor binding process [18–22].

The most remarkable differences between P2X$_1$ and P2X$_3$ receptors are elucidated by the comparison of thermodynamic

data. Interestingly, $P2X_1$ and $P2X_3$ purinergic receptors have a different thermodynamic behavior as demonstrated by the fact that agonists and antagonists for $P2X_1$ receptors show similar enthalpy and entropy values. On the contrary, $P2X_3$ receptors can be considered thermodynamically discriminated because agonist binding is enthalpy and entropy-driven and antagonist binding is totally entropy-driven.

Another observation on purinergic ligands studied is represented by a higher affinity versus $P2X_3$ than versus $P2X_1$ receptors. High affinity values, in the nanomolar range, were found for αβmeATP in both purinergic receptors studied. The order of potency for $P2X_3$ receptors of the agonists was: αβmeATP > 2meSATP > BzATP > ATP > ADP. Similar potencies were also observed to $P2X_1$ receptors even if all ligands, with the exception of αβmeATP, showed a lower affinity in comparison with that obtained to $P2X_3$ receptors. It should be noted that other examples of binding experiments have been reported by using different agonist or antagonist radioligands [12,15–17]. By using [^{35}S]-ATPαS as a radioligand to label P2X receptors, it was found that in synaptosomal membranes from rat brain cortex, ATP, 2MeSATP and suramin revealed lower K_i values, than those found in our conditions [17]. The same authors reported a clear difference between the binding characteristics of different agonists and antagonists using [^{35}S]-ATPαS or [^{3}H]αβmeATP [17]. Furthermore, different affinity values were found using [^{3}H]-A317491 to label $P2X_3$ receptors expressed in 132N1 human astrocytoma cells [12]. In particular, the main difference in affinity values compared to our data concern the K_i values of the antagonists. In fact, A317491, TNP-ATP and PPADS revealed a higher affinity using [^{3}H]-A317491 instead of [^{3}H]αβmeATP. On the contrary, the affinity values of the agonists were strictly similar using [^{3}H]-A317491 or [^{3}H]αβmeATP as radioligands. Some reports revealed weak correlation between radioligand binding profiles and the functional activity of various P2 ligands [36]. Binding and functional studies reported that P2X receptor agonists with high affinity values in the nanomolar range also showed very low potency [37]. In addition, differences in P2X binding parameters could be attributed to various additional factors. In particular it was found that several divalent and trivalent cation salts markedly increase binding of αβmeATP [38]. Some discrepancies between our and previous data might be related either to a different radioligand used to reveal P2X purinergic receptors or to a various cells or tissues expressing purinergic receptors. Some differences are also present by using human or rat purinergic tissues suggesting a species diversity despite their high homology [16]. In our experimental conditions suramin analogs such as NF 023 and NF 279 revealed affinity values in the micromolar range for both purinergic subtypes even if they have been reported be selective for $P2X_1$ receptors [39]. This is probably due to the various experimental conditions used and may also be complicated by the fact that functional P2X ligand-gated ion channels exist as oligomeric combinations with specific subunit arrangements [1,2,11,39]. Interestingly, TNP-ATP a typical nucleotide with a ribose-substituted trinitrophenyl group, defined to be an antagonist in functional assays, behaves in our experimental thermodynamic conditions as an agonist. It is possible to hypothesize that TNP-ATP could interact with the site occupied by the agonists. Another possible explanation could be that the binding of TNP-ATP is present to an allosteric site on a large extracellular region of the receptor representing a common domain that interacts with the strongly electronegative trinitrophenyl moiety [13,40].

More generally, the present study demonstrates that thermodynamic parameters reflect a common mechanism of ligand–receptor interaction and emphasizes the possibility to obtain information about the agonist-antagonist discrimination by simple *in vitro* binding experiments. Thus, analysis of thermodynamic data of drug–receptor interactions appears to be an effective tool for investigating, at a molecular level, the role played during the binding of the ligands. These novel research could be of interest in the identification of novel and potent $P2X_1$ and $P2X_3$ purinergic ligands.

Acknowledgement

Alice Tosi was financially supported by A.F.M. Farmacie Comunali of Ferrara

REFERENCES

[1] North RA. Molecular physiology of P2X receptors. Physiol Rev 2002;82:1013–67.
[2] North RA, Surprenatant A. Pharmacology of cloned P2X receptors. Ann Rev Pharmacol Toxicol 2000;40:563–80.
[3] Burnstock G. Purinergic signalling. Br J Pharmacol 2006;147:172–81.
[4] Sawynok J. Adenosine and ATP receptors. Handb Exp Pharmacol 2007;177:309–28.
[5] Khakh BS, North RA. P2X receptors as cell surface ATP sensors in health and disease. Nature 2006;442: 527–32.
[6] Burnstock G, Knight GE. Cellular distribution and functions of P2 receptor subtypes in different systems. Int Rev Cytol 2004;240:31–4.
[7] Kennedy C. P2X receptors: targets for novel analgesics? Neuroscientist 2005;11:345–56.
[8] Jarvis MF. Contribution of $P2X_3$ homomeric and heteromeric channels to acute and chronic pain. Expert Opin Ther Targets 2003;7:513–22.
[9] Abbracchio MP, Williams M, editors. Handbook of experimental pharmacology purinergic and pirimidinergic signaling, vol. 151 (I and II). Berlin: Springer; 2001.
[10] King BF, North RA, editors. Purine and the autonomic nervous system: from controversy to clinic. J Auton Nerv Syst 2000;81:1–299.
[11] Jacobson KA, Jarvis MF, Williams M. Purine and pyrimidine (P2) receptors as drug targets. J Med Chem 2002;45:4057–93.
[12] Jarvis MF, Bianchi B, Uchic JT, Cartmell J, Lee C-H, Williams M, et al. [^{3}H]A-317491, a novel high affinity non-nucleotide antagonists that specifically labels human $P2X_{2/3}$ and $P2X_3$ receptors. J PET 2004;310:407–16.
[13] Burgard EC, Niforatos W, Van Biesen T, Lynch KJ, Kage KL, Touma E, et al. Competitive antagonism of recombinant $P2X_{2/3}$ receptors by 2′,3′-O-(2,4,6-trinitrophenyl)adenosine 5′-triphosphate (TNP-ATP). Mol Pharmacol 2000;58:1502–10.
[14] Bo X, Burnstock G. High- and low- affinity binding sites for [^{3}H]αβmeATP in rat urinary bladder membranes. Br J Pharmacol 1990;101:291–6.
[15] Michel AD, Chau N-M, Fan T-PD, Frost EE, Humphrey PPA. Evidence that [^{3}H]αβmeATP may label an endothelial-derived cell line 5′-nucleotidase with high affinity. Br J Pharmacol 1995;115:767–74.

[16] Michel AD, Lundstrom K, Buell G-N, Surprenatant A, Valera S, Humphrey PPA. The binding characteristics of human bladder recombinant P2X purinoceptor, labelled with [^{3}H]αβmeATP, [^{35}S]ATPγS or [^{33}P]ATP. Br J Pharmacol 1996;117:1254–60.
[17] Schafer R, Reiser G. Characterization of [^{35}S]ATPαS and [^{3}H]αβmeATP binding sites in rat brain cortical synaptosomes: regulation of ligand binding by divalent cations. Br J Pharmacol 1997;121:913–22.
[18] Borea PA, Dalpiaz A, Varani K, Gilli P, Gilli G. Can thermodynamic measurement of receptor binding yield information on drug affinity and efficacy? Biochem Pharmacol 2000;60:1549–56.
[19] Borea PA, Dalpiaz A, Varani K, Gessi S, Gilli G. Binding thermodynamics at A_1 and A_{2A} adenosine receptors. Life Sci 1996;59:1373–88.
[20] Borea PA, Varani K, Gessi S, Gilli P, Gilli G. Binding thermodynamics at the human neuronal nicotine receptor. Biochem Pharmacol 1998;55:1189–97.
[21] Merighi S, Varani K, Gessi S, Klotz KN, Leung E, Baraldi PG, et al. Binding thermodynamics at the human A_3 adenosine receptors. Biochem Pharmacol 2002;63:157–61.
[22] Gilli P, Gilli G, Borea PA, Varani K, Scatturin A, Dalpiaz A. Binding thermodynamics as a tool to investigate the mechanisms of drug–receptor interactions: thermodynamics of cytoplasmic steroid/nuclear receptors in comparison with membrane receptors. J Med Chem 2005;48:2026–35.
[23] Maksai G. Thermodynamics of ionotropic GABAA, Glycine and 5-HT3 type serotonin receptor interactions. In: Raffa RB, editor. Drug receptor thermodynamics: introduction and applications. New York: Wiley & Sons; 2001. p. 359–76.
[24] Gessi S, Dalpiaz A, Varani K, Borea PA. Temperature dependence and GABA modulation of βcarboline binding to rat cerebellum benzodiazepine receptors. Life Sci 1999; 185–92.
[25] Borea PA, Varani K, Gessi S, Merighi S, Dalpiaz A, Gilli P, et al. Receptor binding thermodynamics at the neuronal nicotinic receptors. Curr Top in Med Chem 2004;4:361–8.
[26] Stoop R, Surprenant A, North RA. Different sensitivities to pH of ATP induced currents at four cloned P2X receptors. J Neurophysiol 1997;78:1837–40.
[27] Froldi G, Varani K, Chinellato A, Ragazzi E, Caparrota L, Borea PA. P_{2x}-purinoceptors in the heart: actions of ATP and UTP. Life Sci 1997;60(17):1419–30.
[28] Borea PA, Dalpiaz A, Varani K, Guerra L, Gilli G. Binding thermodynamics at A_{2A} receptor ligands. Biochem Pharmacol 1995;49:461–9.
[29] Bradford MM. A rapid and sensitive method for the quantitation of microgram quantities of protein utilizing the principle of protein dye-binding. Anal Biochem 1976;72:248.
[30] Munson PJ, Rodbard D. Ligand: a versatile computerized approach for the characterization of ligand binding systems. Anal Biochem 1980;107:220–39.
[31] Gilli P, Ferretti V, Gilli G, Borea PA. Enthalpy–entropy compensation in drug–receptor Binding. J Phys Chem 1994;98:1515–8.
[32] Grunwald E, Steel C. Solvent reorganization and thermodynamic enthalpy–entropy compensation. J Am Chem Soc 1995;117:5687–92.
[33] Raffa RB. In: Raffa RB, editor. Drug–receptor thermodynamics: introduction and applications. New York: Wiley & Sons; 2001. p. 221–416.
[34] Lorenzen A, Guerra L, Campi F, Lang H, Schwabe U, Borea PA. Thermodynamically distinct high and low affinity states of the A(1) adenosine receptor induced by G protein coupling and guanine nucleotide ligation states of G proteins. Br J Pharmacol 2000;130(3):595–604.
[35] Tomlinson E, Steel C. Solvent reorganization and thermodynamic enthalpy–entropy compensation. J Am Chem Soc 1983;13:115–44.
[36] Yu HX, Bianchi B, Metzger R, Lynch KJ, Kowaluk EA, Jawis MF, et al. Lack of specificity of (^{35}S)-ATPγS and (^{35}S)-ADPβS as radioligand for ionotropic and metabotropic P2 receptor binding. Drug Dev Res 1999;48:84–93.
[37] Lambrecht G. Agonists and antagonists acting at P2X receptors: selectivity profiles and functional implications. Naunyn Schmiedebergs Arch Pharmacol 2000;362: 340–50.
[38] Michel AD, Humphrey PP. Effects of metal cations on [^{3}H]alpha,beta-methylene ATP binding in rat vas deferens. Naunyn Schmiedebergs Arch Pharmacol 1994;350: 113–22.
[39] Burnstock G. Physiology and pathophysiology of purinergic neurotransmission. Physiol Rev 2007;87:659–797.
[40] Virginio C, Robertson G, Surprenant A, North RA. Trinitrophenyl-substituted nucleotides are potent antagonists selective for $P2X_1$, $P2X_3$ and heteromeric $P2X_{2/3}$ receptors. Mol Pharmacol 1998;53:969–73.